For. Stud. China, 2007, 9(1): 33–38
DOI 10.1007/s11632-007-0006-2

RESEARCH ARTICLE

Microfibril angle variability in Masson Pine (*Pinus massoniana* Lamb.) using X-ray diffraction

Zhang Bo[1] *Fei Ben-hua*[1*] *Yu Yan*[2] *Zhao Rong-jun*[1]

[1]Research Institute of Wood Industry, Chinese Academy of Forestry, Beijing 100091, P. R. China
[2]International Center for Bamboo and Rattan, Beijing 100102, P. R. China

Abstract The microfibril angle of fiber walls is an ultra-microscopic feature affecting the performance of wood products. It is therefore essential to get more definitive information to improve selection and utilization. X-ray diffraction is a rapid method for measuring microfibril angles. In this paper, the variability of microfibril angle in plantation-grown Masson pine was investigated by peak-fitting method. This method was compared with the traditional hand-drawn method, 40% peak height method and half peak height method. X-ray diffraction measurements indicated that the microfibril angle changed as a function of the position in the tree. The mean microfibril angle decreased more gradually as the distance increased from the pith and reached the same level in mature wood. The microfibril angle also seemed to decrease clearly from the base upward. Differences of angle-intensity curves between heartwood and sapwood were also examined.

Key words X-ray diffraction, microfibril angle, peak-fitting method, half peak height method, Masson pine

1 Introduction

The arrangement of cellulose microfibrils within different cell wall layers of wood fibers is closely related to the physical and mechanical properties of both solid wood and pulp fibers (Cave and Walker, 1994). Since about 70% of the thickness of the fiber wall belongs to the S_2 layer of the fiber, the orientation of the cellulose microfibrils in this layer has a strong effect on the mechanical properties of fibers. When the microfibril angle is large, longitudinal shrinkage increases dramatically (Meylan and Butterfield, 1972). Furthermore, breaking strength, stiffness and dimensional stability all decrease as the microfibril angle increases (Evans and Ilic, 2001). It has been suggested that the variation of this angle might be genetically controlled. The fibril angle is known to be greater in juvenile wood than in mature wood for coniferous species. Thus, the angle of the fibril is not only an important parameter in determining wood and fiber quality but may also be used to define the zone of juvenile wood. Microfibril angles have been shown to play an important role in keeping the developing stem mechanically stable under changing environmental conditions (Booker and Sell, 1998; Lichtenegger et al., 1999). It is therefore of interest to have a better knowledge of the variation in the fibril angle of wood fibers.

X-ray diffraction is a well-established method for determining microfibril angles (Cave, 1966, 1997a, 1997b). Many other methods, such as polarized light (Donaldson, 1991; Ye and Sundstrom, 1997), iodine crystals (Senft and Bendtsen, 1985), sonication (Huang, 1995; Wang et al., 2001) and soft-rot induced cavities (Anagnost et al., 2000) are also used. More recently confocal microscopy (Batchelor et al., 1997; Bergander et al., 2002), transmission electron microscopy (TEM) (Abe et al., 1992) and field emission scanning electron microscopy (FE-SEM) (Abe et al., 1991; Prodhan et al., 1995) have also been reported. Most of these methods, however, are destructive, tedious and time-consuming and thus not applicable for large sets of samples. To study S_2 microfibril angle variations in terms of tree growth conditions, more easily available techniques are needed. Since the pioneering X-ray studies of Cave (1966) and Meylan (1967), a great number of papers on the use of wide angle X-ray diffraction (WAXD) and small angle X-ray scatter (SAXS) from the 002 as well as the 040 planes of cellulose in wood for determining the microfibril angle have been published (Paakkari and Serimaa, 1984; Jakob et al., 1994; Sahlberg et al., 1997; Reiterer et al., 1998). More recently, Evans (1999) and others (Cave, 1997; Entwistle and Navaremjan, 2001; Lichtenegger et al., 2001; Saren et al., 2005) have done extensive work to refine X-ray diffraction as a much more rapid technique for measuring microfibril angles.

In this study we investigated the variability of microfibril angles in annual rings of Masson pine using X-ray diffraction. For our calculations, Gaussian functions were used to analyze the 002 diffraction arc. With the aid of this method, differences of angle-intensity curves between heartwood and mature wood were also discussed.

*Author for correspondence. E-mail: fbh@forestry.ac.cn

2 Materials and methods

2.1 Specimen preparation

The wood samples used in this investigation came from approximately 30-year-old Masson pine (*Pinus massoniana* Lamb.) trees, located at Pingxiang in southern China (22°06′58″ N, 106°43′33″ E, elevation 300 m above sea level). Five sample trees were felled and 15-cm-thick transverse discs were taken at different heights (0, 3, 6 and 9 m) of the stems. After air-drying, 15-cm-wide blocks were removed along the southern radius of each disc. Each wood block was defect-free, straight-grained with evenly spaced growth rings and true tangential and radial sides. Serial tangential samples, 1 mm thick, in radial direction, 15 mm wide and 30 mm long in longitudinal direction, were cut from the pith to the bark in as many wide growth rings as possible and then marked with tree number, growth ring number, height and orientation. The average ring width was 4 mm for plantation grown trees of Masson pine.

2.2 X-ray measurements

A Philips X-ray scattering system (Panalytical X'Pert Pro) was used to collect X-ray diffraction. Each wood sample was attached to a holder that held the wood sample perpendicular to the incident X-ray beam, which passed through the tangential face near the center of the specimen. The sample was rotated and the intensity curve was measured as a function of the rotation angle φ with a step of 0.5° and a measuring time of 180 s per point. The radiation source was a CuKa, with λ = 0.154 nm, 40 kV, 40 mA and a 2 mm×4 mm aperture incident beam. The size of the beam and the loading directions of the samples could be changed when necessary.

2.3 Caculation of *T* by curvefitting

The mean fibril angle was determined according to a method developed by Meylan (1967) and Cave (1966), where half the width of the peak, taken from the tangents, is drawn at the points of inflection. A microfibril angle is determined as 0.6*T* method (Stuart and Evans, 1994; Andersson et al., 2000). The method now has been widely used to determine the fibril angle from measurements of the 002 peak made in transmission.

The intensity of the complete two-dimensional diffractogram was recorded digitally and integrated over an azimuth angle with 0.5° resolution over the 002 crystal plane arcs of the diffractogram. A nonlinear least-squares routine based on Cave's equation was used to fit the angle-intensity data to a Gaussian curve (Fig. 1B). The Gaussian profile gives a good fitting to the sides of the diffraction arcs where the inflection points are located. Fitting a single identical Gaussian curve has the effect of averaging the data from both diffraction peaks and removing the noise.

The model was:

$$y = a + b_1 \cdot \exp\left[\frac{-(x-\mu)^2}{2\sigma_1^2}\right] + b_2 \cdot \exp\left[\frac{-(x-\mu-180)^2}{2\sigma_2^2}\right]$$

where a is constant background; μ, μ+180 centers of the first and the second peak, respectively; σ_1, σ_2 half-widths at inflection points; b_1, b_2 heights of curves above constant background. The T value was estimated as $\sigma_1+\sigma_2$ for the two-peak model and as 2σ for the single peak model. Microfibril angle values were estimated from equation MFA=0.6*T*, where MFA is the microfibril angle (Cave, 1966; Stuart and Evans, 1994). As well, traditional calculation methods are shown in Fig. 1A; for more details see Ruan et al. (1982).

3 Results and discussion

3.1 Scan characteristics

In Fig. 2, three typical scatter diagrams are displayed.

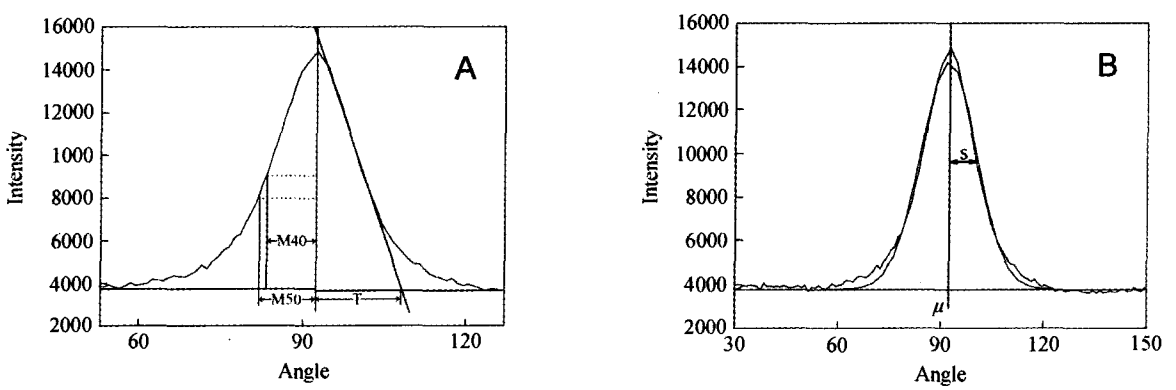

Fig. 1 Measurement of 002 diffraction parameters. A: traditional hand-drawn method, 40% peak height method and half peak height method; B: peak fitting method with Gaussian curve.

Figure 2A shows a typical scatter diagram from mature wood. It consists of a strong single peak indicating small fibril angles. In those cases the data fit a single Gaussian curve very well. Scatter diagrams of rings closest to the pith usually look like Fig. 2B, with wide and flat peaks. Quite a few of the rings closest to the pith also show multiple peaks (Fig. 2C). Obviously, the data in Fig. 2B as well as in Fig. 2C, with higher-angle and noisier signals, do not follow a single Gaussian curve. This does not preclude fitting these models and obtaining estimates of microfibril angles. The fibril angles in juvenile wood were higher than those in mature wood. The resulting flat or multiple peaks shown in Figs. 2B and 2C could, theoretically, be fitted with two Gaussian curves (Fratzl et al., 1997), except in a few cases where the fit with two Gaussians yielded unreasonable results.

To ensure that multiple scattering is small or even negligible, we measured several samples of different thicknesses. Good fits were obtained using 1-mm-thick samples, which means that there were about 1,000 tracheids to a beam of 2 mm×4 mm diameter with more than 3×10^9 independent cellulose crystallites capable of reflecting radiation (Jakob et al., 1994; Cave, 1997). Typical scatter diagrams of 80-μm-thick samples are also shown in Fig. 2D, with noisier signals and higher variability.

3.2 Comparison of different methods

The traditional calculation methods used were a hand-drawn method based on 0.6*T*, a half peak height method and a 40% height method (Ruan et al., 1982). We used a peak-fitting method in our X-ray diffraction calculation. The results of X-ray diffraction diagram of each sample, as measured by the method described above, were compared with the values obtained by our peak-fitting method using a regression analysis program.

Figure 3 shows the linear relationship and regression equations of microfibril angles as measured by our peak-fitting method, the hand-drawn method, the 40% peak height method and the half peak fitting method. The results obtained used the same samples. Sixty samples were used and the coefficients of determination were all above 0.98, which are all significant at the 0.01 level.

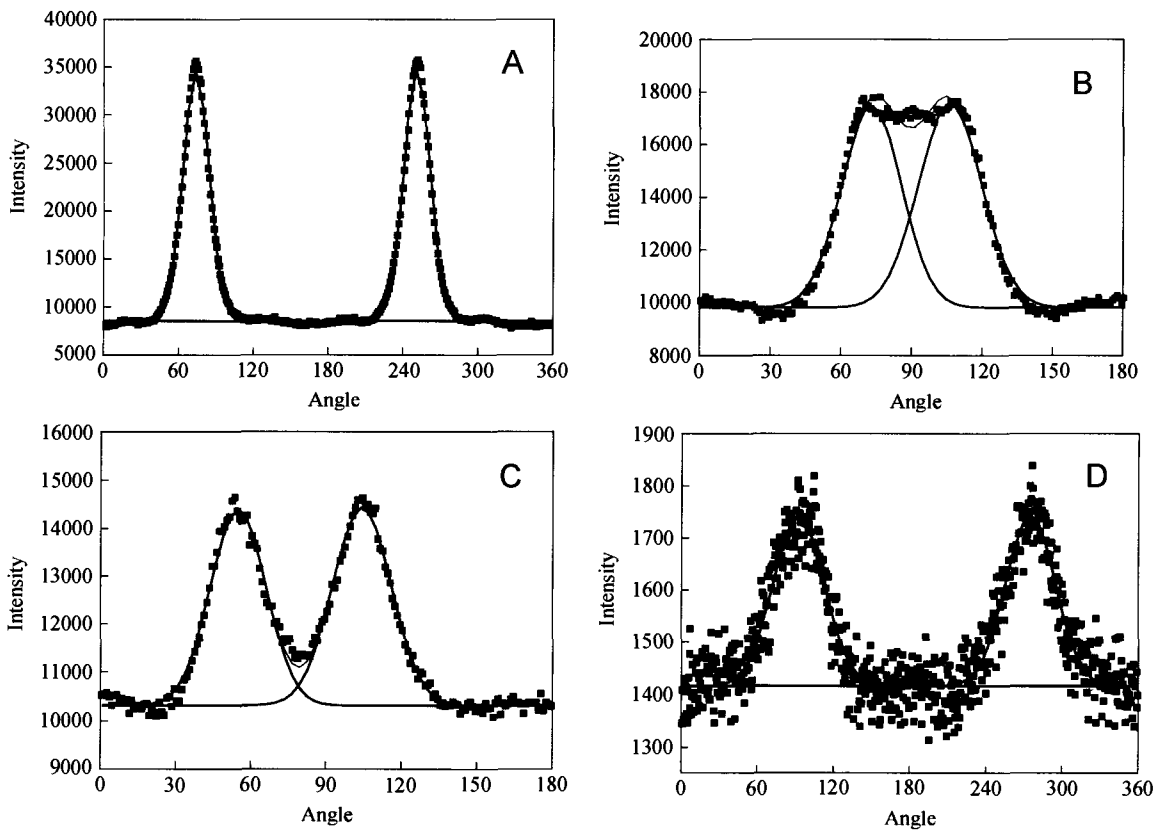

Fig. 2 Intensity variation round the 002 diffraction circle for a Masson pine specimen with an X-ray beam. Since the diffraction patterns from X-rays are, in principle, symmetric, only one half of the pattern needs to be evaluated. The continuous curve represents a least-squares fitting of the data using Gaussian curves. In (A) the scatter pattern obtained from the 20th ring, yielded a narrow peak and could be fitted with a single Gaussian curve. In (B) and (C) from the ring near the pith (4th ring and 3rd ring), the pattern could be fitted with two Gaussian curves of equal width. Samples thickness of A, B and C was 1 mm. In (D) the curve was obtained with 80-μm-thick sample.

Table 1 shows average values comparing microfibril angles calculated using these methods. These methods give angles which differ by less than 2°. It has been shown that in commonly used methods the microfibril angle agrees well with the peak-fitting method. Generally, hand-drawn methods and the 40% peak height give a higher value for microfibril angles.

Thus it seems from this comparison that use of the peak-fitting method for determining microfibril angle is reasonable and indicates that the calibration curve based on this technique for interpreting the X-ray diagram can be used with confidence.

3.3 Microfibril angle variation

In Fig. 4, the fibril angle determined by X-ray diffraction is shown as a function of the annual ring from the pith to the cambium. Plots are arranged side by side for comparison: 3 m height (Fig. 4A), 6 m height (Fig. 4B), 9 m height (Fig. 4C) and base wood at 0 m height (Fig. 5). It is clear, with the exception of the base (0 m), that the microfibril angle decreases from pith to bark. There were, however, differences regarding the detailed course of microfibril angles with increasing stem height.

At 3 m height (Fig. 4A), the microfibril angle decreased from about 30° near the pith to 22° at ring nine and then stayed approximately constant. The data were generally fitted with two Gaussian curves, except

Table 1 Average values of microfibril angle calculated by different methods

Calculation methods	Peak fitting	Hand-drawn	Half peak height	40% peak height
Average value	12.5°	12.9°	11.7°	13.9°

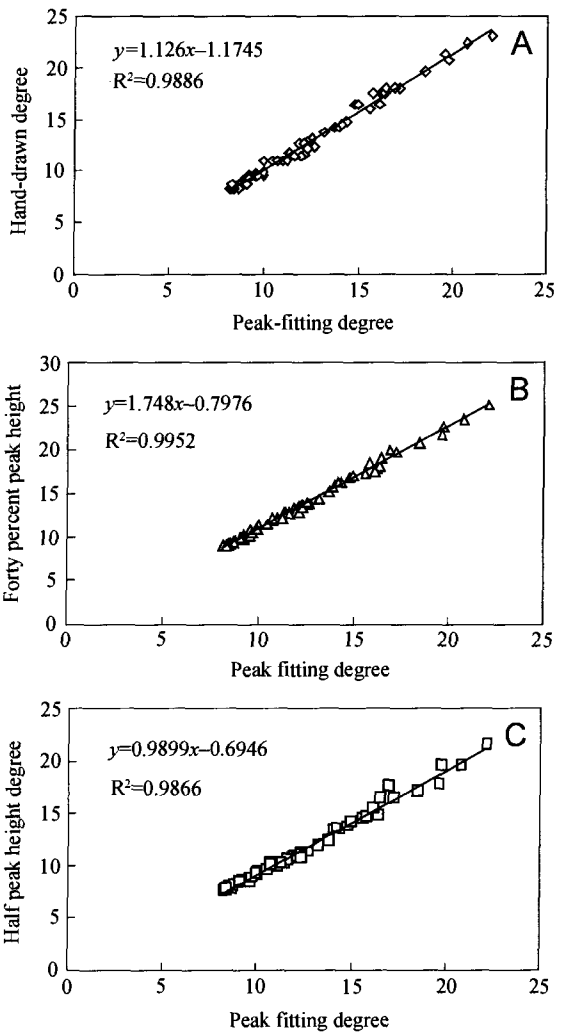

Fig. 3 The relationship between the microfibril angle as measured by three calculation methods. A: measured by peak fitting method and traditional hand-drawn method; B: measured by peak fitting method and half peak height method; C: measured by peak fitting method and 40% peak height method.

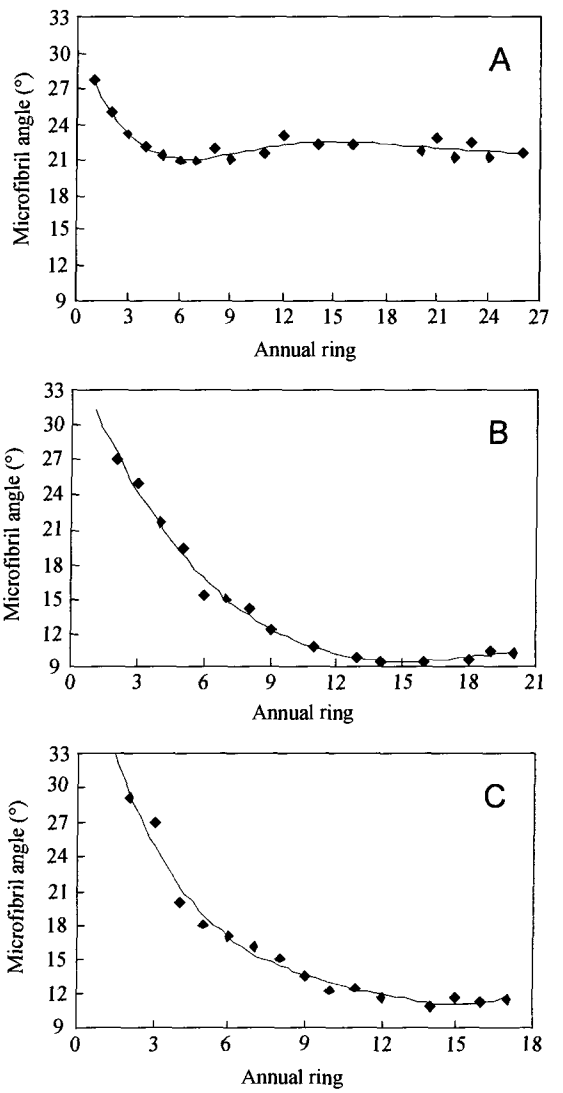

Fig. 4 Mean fibril angle as determined by X-ray diffraction on the 002 reflection as a function of annual rings at distances of 3, 6 and 9 m above ground. A: 3 m; B: 6 m; C: 9 m.

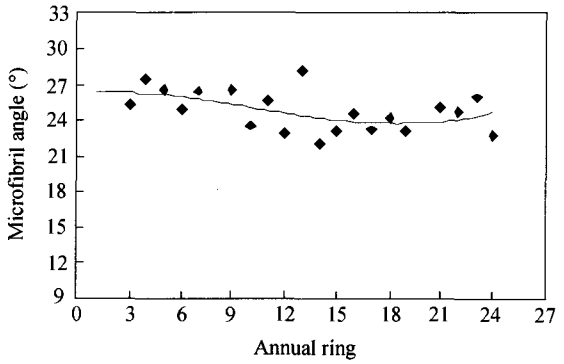

Fig. 5 Mean fibril angle as determined by X-ray diffraction on the 002 reflection as a function of annual ring at distances of base wood (0 m height)

in a few cases where the fit with two Gaussian curves yielded unreasonable results. In Figs. 4B and 4C, the decrease of the microfibril angle from the pith toward the bark was more gradual than that in Fig. 4A. In contrast to Fig. 4A, the microfibril angles stayed at a constant 10° after the 9th ring, much lower than those at 3 m height.

In Fig. 5 (0 m height), the microfibril angle calculated from the scatter signal was generally high, even near the bark, where it was still found to be around 25° and the distribution width was also larger. The microfibril angle stayed constant over the same height.

Although there are great differences among the different locations in wood, in particular between juvenile wood and mature wood, we observed a consistent trend of the mean microfibril angle to decrease from pith to bark, with the exception of 0 m height, where the microfibril angle distribution was found to be constantly high for all annual rings. However, in juvenile wood the microfibril angles were significantly higher than those in the mature wood, not only at 3 m height, where they reached up to 30°. In contrast, the microfibril angles decreased to around 20° in sapwood and even to about 10° at 6 m and 9 m height and still retained the same values in the outer part of the stem. Similar trends for the microfibril angle have also been reported by Sahlberg et al. (1997) and Lichtenegger et al. (1999) for Norway spruce. The 0.6T method, also applied by Sahlberg and Lichtenegger (Cave, 1966), is valid. The trends of the average microfibril angle obtained are in reasonably good agreement with the values of Lichtenegger et al. (1999). However the arrangement of microfibril angle values observed in our study was slightly greater than that reported by Bao and Jiang (1997). Bao and Jiang (1997) found microfibril angles ranging from 10° to 15° in heartwood and from 9° to 10° in sapwood of Masson pine.

The systematic tendency for microfibril angles to decrease from pith to bark, identified by various authors, agree with the results from our work. Saranpaa et al. (1998) showed that in Norway spruce wood microfibril angles decrease from pith to bark according to a curvilinear, possibly an exponential model. Normally the central region of the log is a critical zone, since it consists of juvenile wood which can cause processing problems, such as increasing longitudinal shrinkage and distortion in kiln-dried lumber. Thus, a possible strategy for genetic improvement might be to concentrate efforts on reducing microfibril angles in this region. According to Zobel and van Buijtenen (1989) and Myszewski et al. (2004), the microfibril angle is under moderate genetic control. In addition, Shupe et al. (1996) also showed that fertilizer treatment led to a significant effect on microfibril angle orientation. Meanwhile, many authors (Mattheck and Kubler, 1995; Lichtenegger et al., 1999) still argued that the microfibril angle is controlled by physical forces (gravitational forces, lateral forces) acting on the plasma membrane (via microtubule orientation). These studies therefore suggest that the microfibril angle in standing trees will depend not only on the genotype of the tree, but also on environmental conditions. A more detailed study, between and within growth rings, combined with growing conditions, is necessary so that the pattern of variation in microfibril angle in plantation grown Masson pine wood can be described accurately.

4 Conclusions

The method we have proposed using X-ray diffraction has been shown to be capable of yielding microfibril angle values. By the peak-fitting method we can determine the shape of the microfibril angle distribution. Results indicate that the microfibril angle decreased rapidly up to the 10th year ring and did not change much after that toward the bark. In juvenile wood the microfibril angles were significantly higher than those in mature wood, with the exception of the 0 m height, where the microfibril angle distribution was found to be constantly high for the whole year ring. More detailed studies combined with growing conditions are necessary so that the pattern of variation in microfibril angle in plantation grown Masson pine wood can be described more accurately.

Acknowledgements

This study was financially supported by the National Natural Science Foundation of China (Grant Nos. 30371125 and 30400337).

References

Abe H, Ohtani J, Fukazawa K. 1991. FE-SEM observations on the microfibrillar orientation in the secondary wall of tracheids. IAWA Bull., 12: 431–438

Abe H, Ohtani J, Fukazawa K. 1992. Microfibrillar orientation

of the innermost surface of conifer tracheid walls. IAWA J., 13: 411–417

Anagnost S E, Mark R E, Hanna R B. 2000. Utilization of soft-trot cavity orientation for the determination of microfibril angle. Wood Fiber Sci., 32(1): 81–87

Andersson S, Serimaa R, Torkkeli M, Paakkari T, Saranpaa P, Pesonen E. 2000. Microfibril angle of Norway spruce compression wood: Comparison of measuring techniques. J. Wood Sci., 46: 343–349

Bao F C, Jiang Z H. 1997. The Properties of Wood from Plantations of the Main Tree Species in China. Beijing: China Forestry Publishing House, 36–49

Batchelor W J, Conn A B, Parker I H. 1997. Measuring the fibril angle of fibers using confocal microscopy. Appita J., 50: 377–380

Bergander A, Brandstrom J, Daniel G, Salmen L. 2002. Fibril angle variability in earlywood of Norway spruce using soft rot cavities and polarization confocal microscopy. J. Wood Sci., 48: 255–263

Booker R E, Sell J. 1998. The nanostructure of the cell wall of softwoods and its functions in a living tree. Holz als Roh-und Werkstoff, 58: 1–8

Cave I D. 1966. Theory of X-ray measurement of microfibril angle in wood. For. Prod. J., 16: 37–42

Cave I D, Walker J C F. 1994. Stiffness of wood in fast-grown plantation softwood: the influencc of microfibril angle. For. Prod. J., 44(5): 43–48

Cave I D. 1997a. Theory of X-ray measurement of microfibril angle in wood (part 1). Wood Sci. Technol., 31: 143–152

Cave I D. 1997b. Theory of X-ray measurement of microfibril angle in wood (part 2). Wood Sci. Technol., 32: 225–234

Donaldson L A. 1991. The use of pith apertures as windows to measure microfibril angle in chemical pulp fibers. Wood Fiber Sci., 23: 290–295

Entwistle K M, Navaremjan N. 2001. X-ray diffraction from cellulose micro-fibrils in the S2 layers of structurally characterized softwood specimens. J. Mat. Sci., 36: 3,855–3,863

Evans R. 1999. A variance approach to the X-ray diffractometric estimation of microfibril angle in wood. Appita J., 52: 283–289

Evans R, Ilic J. 2001. Rapid prediction of wood stiffness from microfibril angle and density. For. Prod. J., 51(3): 53–57

Fratzl P, Jakob H F, Rinnerthaler S, Roschger P, Klaushofer K. 1997. Position resolved small-angle X-ray scattering of complex biological materials. J. Appl. Crystallogr., 30: 765–769

Huang C L. 1995. Revealing fibril angle in wood sections by ultrasonic treatment. Wood Fiber Sci., 27: 49–54

Jakob H F, Fratzt P, Tschegg S E. 1994. Size and arrangement of elementary cellulose fibrils in wood cells: a small-angle X-ray scattering study of *Picea abies*. J. Struct. Biol., 113: 13–22

Lichtenegger H, Reiterer A, Stanzl-Tschegg S E, Fratzl P. 1999. Variation of cellulose microfibril angles in softwoods and hardwoods—a possible strategy of mechanical optimization. J. Struct. Biol., 128: 257–269

Lichtenegger H, Reiterer A, Stanzl-Tschegg S E, Fratzl P. 2001. Comment about "The measurement of the micro-fibril angle in soft-wood" by K. M. Entwistle and N. J. Terrill. J. Mat. Sci. Let., 20: 2,245–2,247

Mattheck C, Kubler H. 1995. Wood—The Internal Optimization of Trees. Berlin: Springer-Verlag

Meylan B A. 1967. Measurement of microfibril angle by X-ray diffraction. For. Prod. J., 17(5): 51–58

Meylan B A, Butterfield B G. 1972. The influence of microfibril angle on the longitudinal shrinkage moisture content relationship. Wood Sci. Technol., 6: 293–301

Myszewski J H, Hridgwater F E, Lowe W J, Byram T D, Megraw R A. 2004. Genetic variation in the microfibril angle of loblolly pine from two test sites. SJAF, 28(4): 196–204

Paakkari T, Serimaa R. 1984. A study of the structure of wood cells by X-ray diffraction. Wood Sci. Technol., 18: 79–85

Prodhan A, Funada R, Ohtani J, Abe H, Fukazawa K. 1995. Orientation of microfibrils and microtubules in developing tension-wood fibres of Japanese ash (*Fraxinus mandshurica* var. *japonica*). Planta, 196: 577–585

Reiterer A, Jakob H F, Stanzl-Tschegg S E, Fratzl P. 1998. Spiral angle of elementary cellulose fibrils in cell walls of *Picea abies* determined by small-angle X-ray scattering. Wood Sci. Technol., 32: 335–345

Ruan X G, Yin S C, Sun C Z. 1982. The microfibril angle measurement of the wood fiber secondary walls by X-ray diffraction the methods of the (002) diffraction arc. Sci. Sil. Sin., 18(1): 64–70

Sahlberg U, Salmdn L, Oscarsson A. 1997. The fibrillar orientation in the S2-1ayer of wood fibers as determined by X-ray diffraction analysis. Wood Sci. Technol., 31: 77–86

Saranpaa P, Serimaa R, Andersson S, Pesonen E, Suni T, Paakkari T. 1998. Variation of microfibril angle of Norway spruce and Scots pine—Comparing X-ray diffraction and optical methods. Proceedings of the IUFRO/IAWA International Workshop on the Influence of Microfibril Angle to Wood Quality. Canterbury, New Zealand: University of Canterbury Printers, 240–252

Saren M P, Peura M, Serimaa R. 2005. Interpretation of microfibril angle distributions in wood using microdiffraction experiments on single cells. J. X-ray Sci. Technol., 13: 1–7

Senft J F, Bendtsen B A. 1985. Measuring microfibril angles using light microscopy. Wood Fiber Sci., 17: 564–567

Shupe T F, Choong E T, Stokke D D, Gibson M D. 1996. Variation in cell dimensions and fibril angle for two fertilized even-aged loblolly pine plantations. Wood Fiber Sci., 28: 268–275

Stuart S, Evans R. 1994. X-ray diffraction estimation of the microfibril angle variation in eucalypt wood. Appita, 48(3): 197–200

Wang H H, Drummond J G, Reath S M, Hunt K, Watson P A. 2001. An improved fibril angle measurement method for fibers. Wood Sci. Technol., 34: 439–503

Ye C, Sundstrom O. 1997. Determination of S2-fibril-angle and fiber-wall thickness by microscopic transmission ellipsometry. Tappi J., 80: 181–190

Zobel B J, van Buijtenen J P. 1989. Wood Variation: Its Causes and Control. New York: Springer-Verlag

(Received April 25, 2006 Accepted August 10, 2006)